

Residual Mammographic Microcalcifications and Enhancing Lesions on MRI After Neoadjuvant Systemic Chemotherapy for Locally Advanced Breast Cancer: Correlation with Histopathologic Residual Tumor Size

Young-Seon Kim, MD¹, Jung Min Chang, MD, PhD¹, Hyeong-Gon Moon, MD², Joongyub Lee, MD, PhD³, Sung Ui Shin, MD¹, and Woo Kyung Moon, MD, PhD¹

¹Department of Radiology, Seoul National University College of Medicine, Seoul National University Hospital, Seoul, Korea; ²Department of Surgery, Seoul National University College of Medicine, Seoul National University Hospital, Seoul, Korea; ³Division of Clinical Epidemiology, Medical Research Collaborating Center, Biomedical Research Institution, Seoul National University College of Medicine, Seoul National University Hospital, Seoul, Korea

ABSTRACT

Purpose. To evaluate the accuracy of residual microcalcifications on mammogram (MG) in predicting the extent of the residual tumor after neoadjuvant systemic treatment (NST) in patients with locally advanced breast cancer and to evaluate factors affecting the accuracy of MG microcalcifications using magnetic resonance imaging (MRI) as a reference.

Methods. The patients who underwent NST and showed suspicious microcalcifications on MG comprised our study population. Clinicopathologic and imaging (MG, MRI) findings were investigated. Agreement between image findings and pathology was assessed and factors affecting the discrepancy were analyzed.

Results. Among 207 patients, 196 had residual invasive ductal carcinoma or ductal carcinoma-in-situ (mean size, 3.78 cm). The overall agreement of residual microcalcifications on MG predicting residual tumor extents was lower than MRI in all tumor subtypes (intraclass correlation coefficient [ICC] = 0.368 and 0.723, $p < 0.0001$). The agreement of residual MG microcalcifications and pathology was highest in HR⁺/HER2⁺ tumors and lowest in the triple-negative tumors (ICC = 0.417 and 0.205, respectively). Multivariate linear regression analysis revealed that a size discrepancy between microcalcifications and

histopathology was correlated with molecular subtype ($p = 0.005$). In HR⁺/HER2⁻ and triple-negative subtypes, the mean extents of residual microcalcification were smaller than residual cancer, and overestimation of tumor extent was more frequent in HR⁺/HER2⁺ and HR⁻/HER2⁺ tumors.

Conclusions. The extent of microcalcifications on MG after NST showed an overall lower correlation with the extent of the pathologic residual tumor than enhancing lesions on MRI. The accuracy of residual tumor evaluation after NST with MG and MRI is affected by their molecular subtype.

Neoadjuvant systemic treatment (NST) has long been established as the standard treatment for patients with locally advanced breast cancer (LABC) to downstage the tumor before surgery, as it can render inoperable tumors resectable and increase the rate of breast-conserving therapy in operable cases.¹ Current treatments of patients with LABC target the controls of locoregional disease and micrometastasis.^{2,3} It has also been shown that patients who experience a pathologic complete response (pCR) after neoadjuvant chemotherapy have better long-term survival.⁴⁻⁷

Evaluating the residual tumor size after NST is critical to determine the extent of the operation in breast cancer patients. To date, contrast-enhanced breast magnetic resonance imaging (MRI) is the preferred technique in assessing the residual tumor extent after NST because it is more reliable than conventional methods, such as mammogram (MG) or ultrasound, in the prediction of tumor

size after chemotherapy.^{8,9} However, the optimized use of breast MRI in individual patients receiving NST is still controversial, even though recent studies have focused on identifying various clinical factors that might influence the accuracy of MRI after NST.^{10,11} In addition, there are some limitations in the evaluation of disease extent on MRI for cancers with remaining microcalcifications on MG.¹² To date, data on the histopathologic correlation of MG microcalcifications after NST for LABC remain sparse, and the extent of calcifications on diagnostic MG may not be accurate in the preoperative evaluation of breast cancers after NST.^{12,13} Whether these calcifications reflect residual disease is uncertain, and changes in the number of microcalcifications observed are unreliable indicators of response because not all residual calcifications represent carcinoma.^{14,15}

We hypothesized that the persistence of microcalcifications after NST may not necessarily indicate residual malignant disease, and that patient or lesion variables may affect the MG findings after NST. Therefore, the purpose of this study was to perform a histopathologic correlation of residual microcalcifications on MG after NST in patients with LABC and to evaluate the factors affecting the discrepancy between residual MG microcalcifications and histopathology using MRI as a reference.

MATERIALS AND METHODS

Study Population

This retrospective study was approved by our institutional review board, and the requirement for written informed consent was waived. A search of our database between February 2008 and March 2014 revealed a total of 289 women with stage II or III breast cancers who underwent NST and before surgery. Among them, 207 patients (median age 47 years, range 24–72 years) who had MG performed before and after NST and demonstrated suspicious microcalcifications within the tumor bed available for review, and the results of preoperative MRI were included in this study. Clinicopathologic data and molecular profiles of the studied patients are listed in Table 1.

Preoperative Imaging Technique

MG was performed using dedicated digital MG units (Senographe 2000D, GE Healthcare, Milwaukee, WI; LORAD Selenia, Hologic, Bedford, MA) at the time of breast cancer diagnosis and before starting NST and 1 day before surgery after completion of NST. Standard 2-view MG examinations were performed, and additional views were acquired as deemed necessary.

All patients underwent preoperative breast MRI using a 1.5 T scanner (Signa; GE Medical Systems, Milwaukee, WI) and a dedicated breast coil in the prone position. MRI was performed at a mean of 4.21 days (range 0–25 days) before surgery. After obtaining a bilateral transverse localizer image, fat-suppressed T2-weighted fast spin-echo sagittal images were obtained (repetition time [TR]/echo time [TE], 5500–7150/85.2; image matrix, 256 × 160; field of view, 200 × 200 mm; and section thickness/gap, 1.5 mm/0 mm). A 3-dimensional, T1-weighted fast spoiled gradient-echo sequence was also performed with bilateral sagittal imaging for 1 precontrast and 5 postcontrast dynamic series after 91, 180, 360, 449, and 598 s (TR/TE, 6.5/2.5; flip angle, 10°; image matrix, 256 × 160; field of view, 200 × 200 mm; and section thickness/gap, 1.5 mm/0 mm). The acquisition time of each postcontrast series was 76 s. In all patients, gadobutrol (Gadovist; Bayer Schering Pharma, Berlin, Germany) was injected into the antecubital vein using an automated injector (Spectris Solaris; Medrad Europe, Maastricht, Netherlands) at a dose of 0.1 mmol/kg and at a rate of 2 mL/s, followed by a 20 mL saline flush.

Residual Lesion Evaluation on Preoperative MG and MRI

Preoperative MG and magnetic resonance images were retrospectively evaluated by two radiologists with 7–11 years' experience in breast imaging in consensus masked to the histopathologic, clinical, and imaging findings of other modalities. On MG, the morphology and distribution of microcalcifications were evaluated, and the extent of MG calcifications was measured in centimeters in the greatest dimension. To assess the change in extent, the greatest dimension on the post-NST MG was compared with the pre-NST MG. On MRI, residual enhancing tumor size after NST in the largest dimension was measured.

Pathologic Assessment

Histopathologic evaluation was performed by one pathologist with 20 years' experience in breast pathology. Of the 207 women, 109 (52.7 %) underwent breast-conserving surgery (BCS) or quadrantectomy, and the other 98 (47.3 %) underwent mastectomy. Final histopathology was obtained after surgery at the conclusion of NST. Surgical specimens were sliced into 5 mm thick sections that were fixed in formalin, embedded in paraffin, and stained with hematoxylin and eosin for microscopic evaluation.

pCR was defined as the absence of residual invasive and in-situ cancer.¹⁶ In cases of non-pCR, the largest histopathologic diameters of residual tumors were measured. The expression of estrogen receptor (ER),

TABLE 1 Patient characteristics

Characteristic	Value
Age (year) median (range)	47 (24–72)
Menopausal state	
Premenopausal	96 (46.4 %)
Postmenopausal	111 (53.6 %)
NST regimen	
Anthracycline based	6 (2.9 %)
Taxane plus anthracycline	176 (85.0 %)
Taxane plus trastuzumab	25 (12.1 %)
MG density	
a	5 (2.4 %)
b	30 (14.5 %)
c	129 (62.3 %)
d	43 (20.8 %)
ER	
Positive	115 (55.6 %)
Negative	92 (44.4 %)
PR	
Positive	60 (29.0 %)
Negative	147 (71.0 %)
HER2	
Positive	82 (39.6 %)
Negative	125 (60.4 %)
Molecular subtype	
HR ⁺ /HER2 ⁻	88 (42.5 %)
HR ⁺ /HER2 ⁺	27 (13.0 %)
HR ⁻ /HER2 ⁺	55 (26.6 %)
TN	37 (17.9 %)
Pre-NST clinical T stage	
T1	10 (4.8 %)
T2	83 (40.1 %)
T3	84 (40.6 %)
T4	30 (14.5 %)
Pre-NST clinical N stage	
N0	15 (7.2 %)
N1	102 (49.3 %)
N2	60 (29.0 %)
N3	30 (14.5 %)
Pre-NST microcalcification size (MG) (cm)	3.498 ± 2.572
Post-NST residual microcalcification size (MG) (cm)	3.429 ± 2.709
Post-NST tumor size (MRI) (cm)	3.27 ± 2.2178
Pathologic residual tumor size (cm)	3.7763 ± 2.5573
MG microcalcification—pathology discrepancy (cm)	-0.348 ± 2.961
MRI—pathology discrepancy (cm)	-0.51 ± 1.78

NST neoadjuvant systemic treatment, ER estrogen receptor, PR progesterone receptor, HER human epidermal growth factor receptor, HR hormone receptor (ER or PR), MG mammogram, MRI magnetic resonance imaging, TN triple negative

progesterone receptor (PR), and human epidermal growth factor receptor 2 (HER2) was evaluated by the standard avidin–biotin complex immunohistochemical staining method. A cutoff value of 1 % was used to define ER and PR positivity.¹⁷ HER2 expression was initially assessed by immunohistochemical staining, and tumors with indeterminate HER2 immunohistochemistry results were further evaluated by fluorescence in-situ hybridization (HER2–chromosome 17 centromere ratio >2.0).¹⁸ Using immunohistochemistry, the tumors were classified into the following 4 subtypes according to their hormone receptors (HR [ER or PR]) and HER2 expression statuses: HR⁺/HER2⁻, HR⁺/HER2⁺, HR⁻/HER2⁺, and triple negative (TN) (i.e., ER⁻/PR⁻/HER2⁻).¹⁹

Statistical Analysis

The discrepancies between residual lesion size on MG or MRI and pathologic size (i.e., MG discrepancy = largest dimension of residual microcalcification on MG – residual tumor on histopathology; MRI discrepancy = largest dimension of residual enhancing lesion on MRI – residual tumor on histopathology) were assessed. A 2-tailed Chi square test and Student's *t* test, and multivariate linear regression analysis were used to compare the differences in clinicopathologic variables of the patients that affected size discrepancy. The correlation between the maximum size of the residual microcalcification, enhancing lesions on MRI, and pathology was assessed by intraclass correlation. Intraclass correlation evaluates the ability of a test to discriminate differences among a sample set by comparing the amount of measurement variation with the amount of variation between individuals in the sample.²⁰ Landis criteria were used to interpret intraclass correlation coefficient (ICC) agreement values: slight ($r = 0.00–0.19$), fair ($r = 0.20–0.39$), moderate ($r = 0.40–0.59$), substantial ($r = 0.60–0.79$), and almost perfect ($r = 0.80–1.0$) reliability.²⁰ Comparison of ICC between each modality and pathology was performed by SPSS 22 for Windows (IBM, Armonk, NY). A cutoff value of $p < 0.05$ was considered significant.

RESULTS

Of 207 patients (median age 47 years, range 24–72 years at diagnosis) with LABC who underwent NST, 11 patients (5.3 %) experienced a pCR, and 196 (94.7 %) had residual cancer (mean size, 3.78 cm) (Table 1). On pre-treatment MG, fine pleomorphic or fine linear morphology was most frequently noted in 85 % (176 of 207) of tumors; grouped or segmental distribution was most commonly described in 59.4 % (123 of 207) (Table 2). In the pCR

TABLE 2 Morphology and distribution of calcifications on pretreatment mammogram

Morphology	Distribution					Total
	Regional	Grouped	Linear	Segmental	Diffuse	
Amorphous	3 (1.4 %)	11 (5.3 %)	0	3 (1.4 %)	2 (1.0 %)	19 (9.2 %)
Coarse heterogeneous	5 (2.4 %)	2 (1.0 %)	1 (0.5 %)	4 (1.9 %)	0	12 (5.8 %)
Fine pleomorphic	43 (20.8 %)	45 (21.7 %)	0	31 (15.0 %)	12 (5.8 %)	131 (63.3 %)
Fine linear or linear branching	16 (7.7 %)	10 (4.8 %)	0	17 (8.2 %)	2 (1.0 %)	45 (21.7 %)
Total	67 (32.4 %)	68 (32.9 %)	1 (0.5 %)	55 (26.6 %)	16 (7.7 %)	207

TABLE 3 Residual lesion size and ICC between imaging findings and pathology

Subtype	Histopathologic residual tumor size (cm)	Microcalcification extent on MG (cm)	ICC ^a	MRI enhancing lesion extent (cm)	ICC ^b
All (<i>n</i> = 207)	3.78 ± 2.56	3.43 ± 2.71	0.368	3.27 ± 2.22	0.723
HR ⁺ /HER2 ⁻ (<i>n</i> = 88)	4.58 ± 2.54	3.48 ± 2.74	0.390	3.39 ± 2.23	0.677
HR ⁺ /HER2 ⁺ (<i>n</i> = 27)	3.33 ± 2.63	3.44 ± 2.60	0.417	2.96 ± 2.39	0.797
HR ⁻ /HER2 ⁺ (<i>n</i> = 55)	3.29 ± 2.53	4.01 ± 3.16	0.387	3.34 ± 2.09	0.764
TN (<i>n</i> = 37)	2.91 ± 2.10	2.43 ± 1.57	0.205	3.11 ± 2.32	0.848

ICC intraclass correlation coefficient, MG mammogram, MRI magnetic resonance imaging, HER human epidermal growth factor receptor, HR hormone receptor (estrogen receptor or progesterone receptor), TN triple negative

^a ICC between MG microcalcifications and histopathology

^b ICC between MRI enhancing lesion and histopathology

group, 1 patient had an HR⁺/HER2⁻ tumor, 3 had HR⁺/HER2⁺ tumors, 3 had HR⁻/HER2⁺ tumors, and 4 were TN tumors. Of 11 patients with pCR, microcalcifications on post-NST MG were decreased in five patients (45.5 %) and stable in 6 patients (54.5 %). No patients with pCR had increased microcalcifications on post-NST MG. Of 196 patients with residual tumors, microcalcifications on post-NST MG were decreased in 79 patients (40.3 %), stable in 87 patients (44.4 %), and increased in 30 patients (15.3 %). The residual lesion sizes on MG, MRI, and pathology and the agreements between the image findings and pathology are listed in Table 3. Fair agreement between the pathologic residual tumor size and the extent of residual MG microcalcifications was noted (ICC = 0.368), and substantial agreement was noted between pathologic size and the size of the MRI enhancing lesion (ICC = 0.723).

When the patients were classified according to their tumor subtype, the mean size of microcalcifications on post-NST MG and the pathologic tumor size were as described in Table 3. The agreement of residual MG microcalcifications and pathology was highest in HR⁺/HER2⁺ breast cancer (ICC = 0.417) and lowest in the TN subtype (ICC = 0.205). HR⁺/HER2⁻ breast cancers showed fair agreement between MG microcalcifications

and pathology (ICC = 0.390). Even though the mean size of residual lesion on MG showed closer values to histopathologic measurement than MRI measurement in some subtypes, the ICC values of MRI were higher than those of MG in all subtypes due to standard deviation. The TN subtype showed almost perfect reliability in the prediction of residual tumor extent on MRI (ICC = 0.848), and the HR⁺/HER2⁻ subtype showed substantial reliability in prediction of residual tumor on MRI (ICC = 0.677) (Table 3; Fig. 1).

To identify the independent predictors, the discrepancies between residual lesion size on MG or MRI and pathology were compared in groups of different clinical and pathologic factors (Table 4). Multivariate linear regression analysis revealed that molecular subtype was significantly associated with a discrepancy between MG microcalcifications and pathology (*p* = 0.005). The mean size of residual microcalcifications measured on MG was more likely to exceed the real residual tumor size in HR⁺/HER2⁺ and HR⁻/HER2⁺ tumors, while the measurement of residual microcalcifications on MG tended to be smaller than the pathologic tumor size in HR⁺/HER2⁻ and TN tumors. When measuring the discrepancy between MRI and pathology, molecular subtype and the number of

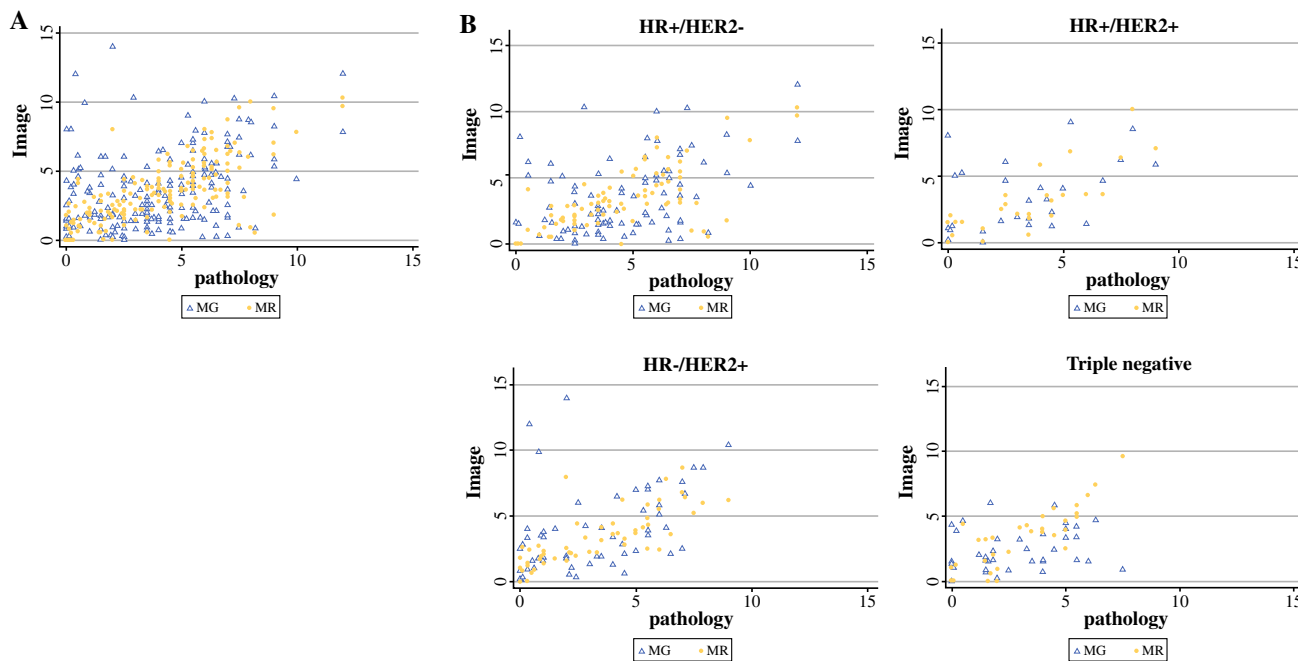


FIG. 1 **a** Overall correlation between image (MG and MRI)-measured residual tumor size and pathologic tumor size. **b** Correlation between image (MG and MRI)-measured tumor size and pathologic

tumor size by molecular subtypes of breast cancer. *MG* mammogram, *MRI* magnetic resonance imaging

neoadjuvant chemotherapy cycles independently affected the difference between MRI and pathology. The mean size of the residual lesion on MRI was underestimated relative to the size of the residual lesion on pathology in the $HR^+/HER2^-$ group ($p < 0.001$) and in the group that received NST more than four times ($p = 0.015$).

DISCUSSION

In this study, we found that the extent of microcalcifications on MG after NST showed overall lower correlation with the extent of the pathologic residual tumor than enhancing lesions on MRI. Among all breast subtypes, $HR^+/HER2^+$ tumors showed the highest agreement between microcalcifications and pathology.

The goal of NST in LABC is to control locoregional disease and micrometastasis.^{2,3,21,22} It can also downstage the tumor before surgery and increase the opportunity to perform BCS instead of mastectomy and reduce the need for axillary lymph node dissection without increasing the risk of locoregional recurrence.^{1,23–25} With the development of new therapeutic agents, rates of pCR to NST have markedly increased; however, a corresponding increase in the rates of BCS has not been observed.^{26–29} Multiple studies have demonstrated the superior accuracy of MRI in evaluating the residual tumor after NST compared to physical examination, MG, and ultrasound.^{30–34} However,

there is little consensus about what should be the appropriate way to evaluate images in patients with NST. In cases of microcalcifications, post-NST MG could be useful to plan the extent of the resection. Furthermore, the presence of residual disease cannot be reliably excluded unless all radiographic abnormalities are removed, even though residual microcalcifications on MG are not always representative of the residual tumor.^{12,13,15,35–37} They may represent treated cancer with calcified or necrotic tissue and sloughed cells in the tumor bed. The changes of MG microcalcifications in breast cancer patients after NST are still confusing and can affect the surgeon's decision as to whether he or she will perform BCS or mastectomy.^{12,13,38}

In several previous studies that evaluated the histopathologic correlation of residual MG microcalcifications after NST, MG microcalcification measurements correlated poorly with tumor size on final pathology.¹³ Similar to our results, MRI was better correlated with the tumor extent, and residual microcalcifications were noted, even in patients with a complete pathologic response.¹³ According to Adrada et al., the extent of calcifications on MG after neoadjuvant chemotherapy does not correlate with the extent of residual disease in up to 22 % of women.¹² In their study, the pCR rate was higher in ER-negative cancers, residual malignant microcalcifications were more frequently noted in ER-positive cancers, and TN cancers had a significantly lower proportion of residual malignant calcifications compared with non-TN cancers.

TABLE 4 Univariate analysis comparing imaging modality pathology discrepancy between subgroups

Parameter	Subgroup	MG		MRI	
		Discrepancy ^a	<i>p</i>	Discrepancy ^b	<i>p</i>
Age	<45 years	-0.29 ± 3.47	0.174	-0.47 ± 2.09	0.834
	≥45 years	-0.60 ± 2.59		-0.52 ± 1.54	
Menopausal	Pre	-0.04 ± 3.28	0.136	-0.50 ± 2.02	0.961
	Post	-0.66 ± 2.67		-0.50 ± 1.55	
ER	Positive	-0.86 ± 2.95	0.008*	-0.99 ± 1.87	0.000*
	Negative	0.24 ± 2.92		1.45 ± 1.87	
PR	Positive	-0.75 ± 3.22	0.244	-0.74 ± 1.80	0.225
	Negative	-0.22 ± 2.88		-0.41 ± 1.77	
HER2	Positive	0.52 ± 3.01	0.000*	-0.09 ± 1.60	0.007*
	Negative	-0.95 ± 2.79		-0.77 ± 1.85	
Molecular subtype	HR ⁺ /HER2 ⁻	-1.10 ± 2.91	0.003	-1.19 ± 1.92	0.000
	HR ⁺ /HER2 ⁺	0.11 ± 2.83		-0.36 ± 1.66	
	HR ⁻ /HER2 ⁺	0.72 ± 3.17		0.04 ± 1.59	
	TN	-0.47 ± 2.35		0.20 ± 1.22	
MG density	a	-1.83 ± 3.56	0.213	0.13 ± 0.49	0.654
	b	-0.46 ± 2.30		-0.58 ± 1.79	
	c	-0.53 ± 2.58		-0.58 ± 1.60	
	d	-0.37 ± 2.98		-0.50 ± 1.78	
NST regimen	Anthracycline based	-0.57 ± 1.55	0.517	-0.62 ± 1.18	0.038*
	Taxane + anthracycline	-0.46 ± 2.99		-0.62 ± 1.76	
	Taxane + trastuzumab	0.27 ± 3.12		0.35 ± 1.82	
T stage	1	1.04 ± 3.59	0.284	0.04 ± 1.85	0.331
	2	-0.27 ± 1.99		-0.31 ± 1.40	
	3	-0.72 ± 3.51		-0.73 ± 2.08	
	4	-0.20 ± 3.29		-0.57 ± 1.75	
N stage	0	-0.54 ± 1.85	0.837	-0.65 ± 0.85	0.484
	1	-0.49 ± 2.67		-0.56 ± 1.69	
	2	-0.34 ± 3.29		-0.60 ± 2.27	
	3	0.06 ± 3.76		-0.04 ± 1.18	
No. of NSTs	<4	-0.60 ± 3.17	0.436	-0.08 ± 1.70	0.015*
	≥4	-0.26 ± 2.88		-0.72 ± 1.79	

MG mammogram, MRI magnetic resonance imaging, ER estrogen receptor, PR progesterone receptor, HER2 human epidermal growth factor receptor 2, NST neoadjuvant systemic treatment, HR hormone receptor (ER or PR), TN triple negative

* Statistically significant

^a Lesion size discrepancy between MG and pathology, calculated by MG subtracted by pathology (MG microcalcifications size – pathologic residual tumor size)

^b Lesion size discrepancy between MRI and pathology, calculated by MRI subtracted by pathology (MRI enhancing lesion size – pathologic residual tumor size)

Regarding the prediction of residual lesions by MRI, we found a higher correlation between MRI and pathology than MG microcalcifications, regardless of tumor subtype. The agreement was highest in TN tumor and lowest in HR⁺/HER2⁻ tumor. In addition, the discrepancy between magnetic resonance-enhancing lesions and pathology was correlated with molecular subtype and the number of NST cycles. In the patients who had HR⁺/HER2⁻ tumors or

patients who received more than four cycles of NST, underestimation of the tumor extent was more frequent. In other recent studies, the accuracy of the prediction of tumor extent with MRI after NST varies with the HR and HER2 status, and similar results were also observed.^{11,39–41} The underlying reason for the higher accuracy of MRI in TN breast cancer can be explained by the distinct vascular characteristics of TN breast cancer, such as higher capillary

permeability.⁴² Taking the results of MG and MRI together, the potential discrepancy between the MG- or MRI-predicted residual tumor size and actual pathologic extent should be considered with the breast cancer subtype, especially when BCS is planned after NST.

In our study, the pCR rate was only 5.3 %, which is much lower than other previous studies. There could be several reasons for this lower pCR rate. All patients included in this study demonstrated suspicious microcalcifications within the tumor bed, and the patients who received NST but did not show microcalcifications were not included. Therefore, the portion of TN cancer that presents as a smooth or circumscribed mass rather than as fine pleomorphic microcalcifications and that has been reported to have a higher pCR rate was relatively lower (17.9 %) than that found in another study (27.7 %).^{10,43,44} In addition, we also included patients who received a short course of NST (<4 cycles). This could be another possible explanation for the low pCR rate.⁴⁵

This study has several limitations. First, this study is a retrospective single-center study with a relatively small number of patients, which was not sufficient to draw specific conclusions for each subtype of breast cancer. Second, patients underwent multiple chemotherapy regimens and different numbers of NST cycles before surgery. Third, most patients did not undergo MRI at diagnosis (before receiving the first dose of chemotherapy), so a comparison of prechemotherapy MG and prechemotherapy MRI was not possible. The evaluation of changes in the tumor after NST on MRI was also not possible. In addition, after chemotherapy, MG and MRI were not performed in the same day, although the time interval between postchemotherapy MRI and MG was not particularly long.

In conclusion, our study demonstrated that the extent of microcalcifications on MG after NST showed fair agreement with the extent of the pathologic residual tumor, and this agreement was lower than that of MRI. The accuracy of the evaluation of tumor extent after NST with MG and MRI is affected by the molecular subtype and the number of NST cycles. Our results demonstrated that the extent of surgery after NST should be carefully and individually determined in patients with different tumor subtypes. MRI information could be more reliable in discerning the tumor extent, and concerns about incomplete excision related to residual calcifications may be less of an issue with certain subtypes of breast cancer. These observations may inform future clinical practice if validated in prospective trials.

ACKNOWLEDGMENT Supported in part by the Seoul National University Hospital Research Fund (Grant 04-2015-0740).

DISCLOSURE The authors declare no conflict of interest.

REFERENCES

1. Kaufmann M, Hortobagyi GN, Goldhirsch A, et al. Recommendations from an international expert panel on the use of neoadjuvant (primary) systemic treatment of operable breast cancer: an update. *J Clin Oncol.* 2006;24:1940–9.
2. Redden MH, Fuhrman GM. Neoadjuvant chemotherapy in the treatment of breast cancer. *Surg Clin North Am.* 2013;93:493–9.
3. Buchholz TA, Lehman CD, Harris JR, et al. Statement of the science concerning locoregional treatments after preoperative chemotherapy for breast cancer: a National Cancer Institute conference. *J Clin Oncol.* 2008;26:791–7.
4. Rastogi P, Anderson SJ, Bear HD, et al. Preoperative chemotherapy: updates of National Surgical Adjuvant Breast and Bowel Project Protocols B-18 and B-27. *J Clin Oncol.* 2008;26:778–85.
5. Jeruss JS, Mittendorf EA, Tucker SL, et al. Combined use of clinical and pathologic staging variables to define outcomes for breast cancer patients treated with neoadjuvant therapy. *J Clin Oncol.* 2008;26:246–52.
6. Symmans WF, Peintinger F, Hatzis C, et al. Measurement of residual breast cancer burden to predict survival after neoadjuvant chemotherapy. *J Clin Oncol.* 2007;25:4414–22.
7. Charfare H, Limongelli S, Purushotham AD. Neoadjuvant chemotherapy in breast cancer. *Br J Surg.* 2005;92:14–23.
8. Chagpar AB, Middleton LP, Sahin AA, et al. Accuracy of physical examination, ultrasonography, and mammography in predicting residual pathologic tumor size in patients treated with neoadjuvant chemotherapy. *Ann Surg.* 2006;243:257–64.
9. Le-Petross HC, Hylton N. Role of breast MR imaging in neoadjuvant chemotherapy. *Magn Reson Imaging Clin N Am.* 2010;18:249–58, viii–ix.
10. Moon HG, Han W, Lee JW, et al. Age and HER2 expression status affect MRI accuracy in predicting residual tumor extent after neoadjuvant systemic treatment. *Ann Oncol.* 2009;20:636–41.
11. Nakahara H, Yasuda Y, Machida E, et al. MR and US imaging for breast cancer patients who underwent conservation surgery after neoadjuvant chemotherapy: comparison of triple negative breast cancer and other intrinsic subtypes. *Breast Cancer.* 2011;18:152–60.
12. Adrada BE, Huo L, Lane DL, Arribas EM, Resetkova E, Yang W. Histopathologic correlation of residual mammographic microcalcifications after neoadjuvant chemotherapy for locally advanced breast cancer. *Ann Surg Oncol.* 2015;22:1111–7.
13. Weiss A, Lee KC, Romero Y, et al. Calcifications on mammogram do not correlate with tumor size after neoadjuvant chemotherapy. *Ann Surg Oncol.* 2014;21:3310–6.
14. Libshitz HI, Montague ED, Paulus DD. Calcifications and the therapeutically irradiated breast. *AJR Am J Roentgenol.* 1977;128:1021–5.
15. Moskovic EC, Mansi JL, King DM, Murch CR, Smith IE. Mammography in the assessment of response to medical treatment of large primary breast cancer. *Clin Radiol.* 1993;47:339–44.
16. von Minckwitz G, Untch M, Blohmer JU, et al. Definition and impact of pathologic complete response on prognosis after neoadjuvant chemotherapy in various intrinsic breast cancer subtypes. *J Clin Oncol.* 2012;30:1796–804.
17. Spitale A, Mazzola P, Soldini D, et al. Breast cancer classification according to immunohistochemical markers: clinicopathologic features and short-term survival analysis in a population-based study from the south of Switzerland. *Ann Oncol.* 2009;20:628–35.
18. Wolff AC, Hammond ME, Hicks DG, et al. Recommendations for human epidermal growth factor receptor 2 testing in breast cancer: American Society of Clinical Oncology/College of

- American Pathologists Clinical Practice Guideline Update. *J Clin Oncol*. 2013;31:3997–4013.
19. Lee HJ, Song IH, Seon AN, et al. Correlations between molecular subtypes and pathologic response patterns of breast cancers after neoadjuvant chemotherapy. *Ann Surg Oncol*. 2015;22:392–400.
 20. Landis JR, Koch GG. The measurement of observer agreement for categorical data. *Biometrics*. 1977;33:159–74.
 21. De Lena M, Zucali R, Viganotti G, Valagussa P, Bonadonna G. Combined chemotherapy–radiotherapy approach in locally advanced (T3b-T4) breast cancer. *Cancer Chemother Pharmacol*. 1978;1:53–9.
 22. Buzdar AU, Montague ED, Barker JL, Hortobagyi GN, Blumenschein GR. Management of inflammatory carcinoma of breast with combined modality approach—an update. *Cancer*. 1981;47:2537–42.
 23. Mieog JS, van der Hage JA, van de Velde CJ. Neoadjuvant chemotherapy for operable breast cancer. *Br J Surg*. 2007;94:1189–200.
 24. Fisher B, Brown A, Mamounas E, et al. Effect of preoperative chemotherapy on local-regional disease in women with operable breast cancer: findings from National Surgical Adjuvant Breast and Bowel Project B-18. *J Clin Oncol*. 1997;15:2483–93.
 25. van der Hage JA, van de Velde CJ, Julien JP, Tubiana-Hulin M, Vandervelden C, Duchateau L. Preoperative chemotherapy in primary operable breast cancer: results from the European Organization for Research and Treatment of Cancer trial 10902. *J Clin Oncol*. 2001;19:4224–37.
 26. Untch M, Loibl S, Bischoff J, et al. Lapatinib versus trastuzumab in combination with neoadjuvant anthracycline–taxane–based chemotherapy (GeparQuinto, GBG 44): a randomised phase 3 trial. *Lancet Oncol*. 2012;13:135–44.
 27. Bear HD, Anderson S, Brown A, et al. The effect on tumor response of adding sequential preoperative docetaxel to preoperative doxorubicin and cyclophosphamide: preliminary results from National Surgical Adjuvant Breast and Bowel Project Protocol B-27. *J Clin Oncol*. 2003;21:4165–74.
 28. Baselga J, Bradbury I, Eidtmann H, et al. Lapatinib with trastuzumab for HER2-positive early breast cancer (NeoALTTO): a randomised, open-label, multicentre, phase 3 trial. *Lancet*. 2012;379(9816):633–40.
 29. Guarneri V, Frassoldati A, Bottini A, et al. Preoperative chemotherapy plus trastuzumab, lapatinib, or both in human epidermal growth factor receptor 2–positive operable breast cancer: results of the randomized phase II CHER-LOB study. *J Clin Oncol*. 2012;30:1989–95.
 30. Hylton NM, Blume JD, Bernreuter WK, et al. Locally advanced breast cancer: MR imaging for prediction of response to neoadjuvant chemotherapy—results from ACRIN 6657/I-SPY TRIAL. *Radiology*. 2012;263:663–72.
 31. Marinovich ML, Houssami N, Macaskill P, et al. Meta-analysis of magnetic resonance imaging in detecting residual breast cancer after neoadjuvant therapy. *J Natl Cancer Inst*. 2013;105:321–33.
 32. Yeh E, Slanetz P, Kopans DB, et al. Prospective comparison of mammography, sonography, and MRI in patients undergoing neoadjuvant chemotherapy for palpable breast cancer. *AJR Am J Roentgenol*. 2005;184:868–77.
 33. Rosen EL, Blackwell KL, Baker JA, et al. Accuracy of MRI in the detection of residual breast cancer after neoadjuvant chemotherapy. *AJR Am J Roentgenol*. 2003;181:1275–82.
 34. Turnbull LW. Dynamic contrast-enhanced MRI in the diagnosis and management of breast cancer. *NMR Biomed*. 2009;22:28–39.
 35. Kwong MS, Chung GG, Horvath LJ, et al. Postchemotherapy MRI overestimates residual disease compared with histopathology in responders to neoadjuvant therapy for locally advanced breast cancer. *Cancer J*. 2006;12:212–21.
 36. Esserman LE, d'Almeida M, Da Costa D, Gerson DM, Poppiti RJ Jr. Mammographic appearance of microcalcifications: can they change after neoadjuvant chemotherapy? *Breast J*. 2006;12:86–7.
 37. Croshaw R, Shapiro-Wright H, Svensson E, Erb K, Julian T. Accuracy of clinical examination, digital mammogram, ultrasound, and MRI in determining postneoadjuvant pathologic tumor response in operable breast cancer patients. *Ann Surg Oncol*. 2011;18:3160–3.
 38. King TA, Morrow M. Surgical issues in patients with breast cancer receiving neoadjuvant chemotherapy. *Nat Rev Clin Oncol*. 2015;12:335–43.
 39. Moon HG, Han W, Ahn SK, et al. Breast cancer molecular phenotype and the use of HER2-targeted agents influence the accuracy of breast MRI after neoadjuvant chemotherapy. *Ann Surg*. 2013;257:133–7.
 40. McGuire KP, Toro-Burguete J, Dang H, et al. MRI staging after neoadjuvant chemotherapy for breast cancer: does tumor biology affect accuracy? *Ann Surg Oncol*. 2011;18:3149–54.
 41. Ko ES, Han BK, Kim RB, et al. Analysis of factors that influence the accuracy of magnetic resonance imaging for predicting response after neoadjuvant chemotherapy in locally advanced breast cancer. *Ann Surg Oncol*. 2013;20:2562–8.
 42. Li SP, Padhani AR, Taylor NJ, et al. Vascular characterisation of triple negative breast carcinomas using dynamic MRI. *Eur Radiol*. 2011;21:1364–73.
 43. Wang Y, Ikeda DM, Narasimhan B, et al. Estrogen receptor–negative invasive breast cancer imaging features of tumors with and without human epidermal growth factor receptor type 2 overexpression. *Radiology*. 2008;246:367–75.
 44. Sanchez-Munoz A, Garcia-Tapiador AM, Martinez-Ortega E, et al. Tumour molecular subtyping according to hormone receptors and HER2 status defines different pathological complete response to neoadjuvant chemotherapy in patients with locally advanced breast cancer. *Clin Transl Oncol*. 2008;10:646–53.
 45. Keam B, Im SA, Kim HJ, et al. Prognostic impact of clinicopathologic parameters in stage II/III breast cancer treated with neoadjuvant docetaxel and doxorubicin chemotherapy: paradoxical features of the triple negative breast cancer. *BMC Cancer*. 2007;7:203.